Remote Sensing in Ecology and Conservation
Open Access
ZSL

RESEARCH ARTICLE

Mapping oil palm plantations and their implications on forest and great ape habitat loss in Central Africa

Mohammed S. Ozigis[1], Serge Wich[1,2], Adrià Descals[3], Zoltan Szantoi[4,5] & Erik Meijaard[6,7,8]

[1]School of Biological and Environmental Sciences, Liverpool John Moores University, James Parsons Building, 3 Byrom Street, Liverpool L3 3AF, UK
[2]Institute for Biodiversity and Ecosystem Dynamics, University of Amsterdam, Science Park 904, 1098 XH, Amsterdam, the Netherlands
[3]CREAF, Cerdanyola del Vallès, 08193, Barcelona, Spain
[4]Science, Applications and Climate Department, European Space Agency, Frascati 00044, Italy
[5]Department of Geography and Environmental Studies, Stellenbosch University, Stellenbosch 7602, South Africa
[6]Durrell Institute of Conservation and Ecology, University of Kent, Canterbury CT2 7NR, UK
[7]School of Biological Sciences, University of Queensland, Brisbane Queensland, 4072, Australia
[8]Borneo Futures, Bandar Seri Begawan BA 2711, Brunei Darussalam

Keywords
Agriculture, deep learning, oil palm, remote sensing, U-Net

Correspondence
Mohammed S. Ozigis, School of Biological and Environmental Sciences, Liverpool John Moores University, James Parsons Building, 3 Byrom Street, Liverpool L3 3AF, UK. E-mail: m.s.ozigis@ljmu.ac.uk

Funding Information
This research was undertaken with financial support from the United Nation Environmental Programme (UNEP) under the Global Environment Facility (GEF) Congo Basin Impact Program (PCA/2022/5067).

Editor: Prof. Nathalie Pettorelli
Associate Editor: Dr Henrike Schulte to Buhne

Received: 4 December 2023; Revised: 6 November 2024; Accepted: 19 November 2024

doi: 10.1002/rse2.428

Abstract

Oil palm (*Elaeis guineensis*) cultivation in Central Africa (CA) has become important because of the increased global demand for vegetable oils. The region is highly suitable for the cultivation of oil palm and this increases pressure on forest biodiversity in the region. Accurate maps are therefore needed to understand trends in oil palm expansion for landscape-level planning, conservation management of endangered species, such as great apes, biodiversity appraisal and supply of ecosystem services. In this study, we demonstrate the utility of a U-Net Deep Learning Model and product fusion for mapping the extent of oil palm plantations for six countries within CA, including Cameroon, Central African Republic, Democratic Republic of Congo (DRC), Equatorial Guinea, Gabon and Republic of Congo. Sentinel-1 and Sentinel-2 data for the year 2021 were classified using a U-Net model. Overall classification accuracy for the final oil palm layer was 96.4 ± 1.1%. Producer Accuracy (PA) and User Accuracy (UA) for the industrial and smallholder oil palm classes were 91.6 ± 1.7% and 95.0 ± 1.3%, 67.7 ± 2.8% and 70.0 ± 2.8%. Post classification assessment of the transition from tropical moist forest (TMF) cover to oil palm within the six CA countries suggests that over 1000 Square Kilometer (km^2) of forest within great ape ranges had so far been converted to oil palm between 2000 and 2021. Results from this study indicate a more extensive cover of smallholder oil palm than previously reported for the region. Our results also indicate that expansion of other agricultural activities may be an important driver of deforestation as nearly 170 000 km^2 of forest loss was recorded within the IUCN ranges of the African great apes between 2000 and 2021. Output from this study represents the first oil palm map for the CA, with specific emphasis on the impact of its expansion on great ape ranges. This presents a dependable baseline through which future actions can be formulated in addressing conservation needs for the African Great Apes within the region.

Introduction

The global demand for vegetable oil has more than doubled in the last two decades following increased demand in the food, cosmetics, and energy sectors (FAO, 2020). While Indonesia and Malaysia contribute most to the global production of and trade in palm oil, other countries, especially in Africa have shown signs of increased oil palm cultivation (Meijaard et al., 2018; Wich et al., 2014). This increased production has a huge impact on the natural forest, biodiversity, conservation, and our ability to mitigate climate change (Alcock et al., 2022).

Agricultural expansion in general and oil palm expansion specifically has implications for Goals 15, 12, and 13, of the Sustainable Development Goals (SDGs), which focuses, respectively, on safeguarding life on land, responsible production and consumption, and climate action, respectively (Meijaard et al., 2018). Recent data from FAOSTAT puts the global total harvested area of oil palm fruit at 289 000 km^2 (FAO, 2022), and a total production figure of 416.4 Million tons (Mt) as at 2021. Results from (Descals et al., 2021) a remote sensing study that mapped oil palm plantations estimates the global area of closed canopy oil palm for both smallholder and industrial oil palm at 210 000 km^2.

Oil palm is regularly favored over other vegetable oil crops due to its high yield and concomitant low land requirements to attain the same production. Palm oil is an important product used in the food industry (in the production of biscuits, cake, margarine, frying fats and chocolate) (Pande et al., 2012), in the cosmetic industry (in the production of soap, shampoo, and cleaning products) (Kalustian, 1985), and in the energy sector (for biofuel) (Lai et al., 2015). Oil palm starts yielding 3 years after planting, then yields increase before plateauing between 7 and 15 years, after which yield declines slowly until the palm needs replacing at around 25–30 years of age (Corley & Tinker, 2008; Danylo et al., 2021). Another special characteristics of oil palm that makes it desirable over other vegetable oil is its ability to grow well and profitably in hemic and sapric peat lands, sands and acid sulfate soils, which are less suitable for other vegetable oil crops (Corley & Tinker, 2016; Meijaard et al., 2018; Naidu, 2006; Veloo et al., 2015). This makes oil palm fruit cultivation a major driver of deforestation, flooding, (Austin et al., 2019; Gaveau et al., 2019; Meijaard & Sheil, 2019; Rodríguez et al., 2021; Wijedasa et al., 2017), loss of biodiversity (Margono et al., 2014), and poor air quality (Noojipady et al., 2017; Van der Werf et al., 2009).

Data from FAO (2022), Meijaard et al. (2018), Wich et al. (2014) suggests an increased rate of palm oil production in CA indicating the need to develop accurate maps of oil palm in the region and assess the impact it has had on land cover change. Particularly the biodiversity rich forest environments of Gabon, Republic of Congo, Democratic Republic of Congo, Cameroon, and Equatorial Guinea (constituting the Congo basin) are potentially at risk from oil palm expansion. The Congo Forest is the second largest forest in the world and plays an important role in carbon sequestration, and biodiversity conservation (Shapiro et al., 2021). Evidence from several studies (Hansen et al., 2013; Shapiro et al., 2022; Vancutsem et al., 2021) suggests that the Congo Forest area has significantly declined in the past four decades. Shapiro et al. (2022) noted that over 2.34 Mha of CA forest cover has been lost to deforestation between 2015 and 2020, for which cropland expansion (including industrial-scale oil palm production and expanding small-scale agriculture) is largely responsible (Curtis et al., 2018; Feintrenie, 2014; Tegegne et al., 2016; Tyukavina et al., 2018). Tyukavina et al. (2018) particularly noted in this regard that small-scale forest clearing for agriculture including for rotational agriculture (82.1 $\pm$ 1.8%) and semipermanent transition of woody vegetation into cropland (2.1 $\pm$ 0.5%), both represents subsistence farming or production of commercial crops are mostly responsible for forest loss in the 15-year period (2000–2014) assessment of the Congo forest.

The CA shelters a tropical rainforest ecosystem with great implication for wildlife and biodiversity. In this study, we focus on assessing the impact of oil palm expansion on great ape range, since great apes are a flagship and umbrella species. Previous studies such as Strona et al. (2018) and Wich et al. (2014) have assessed the impact of oil palm expansion on great ape ranges (GAR) in Africa. But the analyses in these studies relied on land suitability for oil palm cultivation, current land use versus primate distribution, diversity, and vulnerability, as opposed to an actual assessment of mapped oil palm plantations on great ape ranges.

Even though hunting is the main threat to the African great apes, the United Nations Great Apes Survival Partnership (GRASP) initiative and the Section on Great Apes (SGA) of the International Union for Conservation of Nature (IUCN) Species Survival Commission (SSC) reports for 2018 and 2023 have linked the increased extinction risk of these (critically) endangered species to accelerated conversion of forest cover into other land cover types (including villages, agriculture, roads, oil pipeline, logging area, mines and mineral extraction) (GRASP, 2018, 2023). A report by UNESCO (2020) estimated that by 2030, infrastructure development leading to deforestation or habitat fragmentation will have damaged more than 90% of ape habitat in Africa. Likewise, a WWF report, which also noted that the area of forest in this region is expected to decline by 30% in the next 50 years (WWF, 2009). Wich et al. (2014) found that, large parts of these great ape habitats are not protected and at the same time very suitable for oil palm production. No studies have focused on establishing the nexus between forest cover loss, great ape range and oil palm distribution in CA. Developing an accurate oil palm map for CA is therefore essential to understanding the linkage between deforestation, oil palm production and great apes.

To understand trends in oil palm expansion and develop landscape-level planning, accurate maps are

needed to comprehend the rate of change and transition among land cover types. Recent studies using satellite remote sensing and machine learning have produced accurate maps of land cover types (Mhanna et al., 2023; Yomo et al., 2023; Zafar et al., 2024). Several studies have relied on the use of radar satellite images to develop maps for oil palm distribution, for example, Rodríguez et al. (2021) as well as high-resolution (<2.5 m) images in Google Earth (Cheng et al., 2018). Descals et al. (2019) used optical and radar satellite data to map oil palm globally, differentiating between large-holders and smallholders. While some of these studies (Cheng et al., 2018; Descals et al., 2021) have resulted in maps that included oil palm in Africa, no comprehensive mapping has been conducted specifically for the CA. More detailed studies are thus required to increase accuracy at a more regional scale as well as to overcome problems with misclassifications (Descals et al., 2021).

In addition, while the use of machine learning methods including random forest (Breiman, 2001) and support vector machines (Cortes & Vapnik, 1995) has proven to be useful for landcover classification (Adugna et al., 2022; Thanh Noi & Kappas, 2017; Xu et al., 2019) and anormaly detection (Descals et al., 2019; Ozigis et al., 2019, 2020; Su et al., 2021), deep learning algorithms (such as convolutional neural networks) have proven to be more robust than machine learning methods (Shadman Roodposhti et al., 2019). This is because of its intrinsic ability to learn feature shape, dimensions and characteristics automatically from the data which does not require the features to be hand-engineered (Ghosh et al., 2019; Minaee et al., 2021).

This study attempts to bridge this gap by focusing on mapping oil palm specifically for CA. To achieve this, we used a U-Net model trained with Sentinel-1 and Sentinel-2 data over the CA. The model was used to map Industrial Oil Palm (IOP) plantations, Smallholder Oil Palm (SOP) and Other lands (OL). The mapped IOP and SOP (within the IUCN great ape ranges in CA) was compared with forest cover for the year 2000 to establish the extent to which oil palm replaced forest. Lastly, the great ape range was used to determine the extent of forest loss within the different ranges.

Materials and Methods

Study area

This study focused on six countries in CA, which include the Democratic Republic of Congo, Republic of Congo, Gabon, Cameroon, the Central African Republic, and Equatorial Guinea. These countries were chosen because of their location in the Congo Basin, their suitability for oil palm growth and cultivation, and their importance for great apes. The study area (as shown in Fig. 1) had a total area coverage of 3 733 000 km^2 and sits within 7.54° N–9.74° W and 12.81° S–30.43° E. The area has a rich composition of tropical rain forest, mangrove vegetation, cropland, and shrubs, as shown in the land cover map presented. With an annual average temperature ranging from 23°C in the south to 26°C in the north, the region has a tropical, humid equatorial climate in the south and a Sahelo-Sudanian climate in the north (Worldbank, 2020).

Remote Sensing Data (Sentinel-1 and Sentinel-2)

In this study, we used the Sentinel-1 synthetic aperture radar (SAR) Ground Range Detected (GRD) VV and VH polarized products, and the Sentinel-2 Multispectral Instrument (MSI) in the band 4 (red). This is based on results of previous experiments conducted by Descals et al. (2021) highlighting the suitability of the selected image pairs for the delineation of oil palm. We used observations from the two sensors between January and December 2021 to develop a single image composite (Sentinel-1 VV, Sentinel-1 VH, and Sentinel-2 Band 4) for classification. This study used both the Interferometric Wide Swath images and Ground Range Detecting (GRD) products (for both ascending and descending orbits) to generate the final Sentinel-1 mosaic for the year 2021 for the study area. The images were resampled to assume a uniform spatial resolution of 10 m, implemented local incident angle (LIA) correction, after which the median pixel values were used to generate the final single VV and VH mosaic for the study area as implemented in (Descals et al., 2021). In addition, the Sentinel-2 images (comprising of Sentinel-2A and Sentinel-2B) were masked with the quality flag provided in Level 2A, for clouds, cloud shadows, and other non-valid observations (Drusch et al., 2012) using the ATCOR algorithm. The median cloud free surface reflectance band 4 (red band) pixels with a spatial resolution of 10 m was used to generate a single mosaic. The final Sentinel-2 band 4 image was layer stacked with the preprocessed Sentinel-1 VV and VH mosaics to generate a single image composite based on a 100-by-100 km^2 tile for the study area for the year 2021.

Oil palm and forest cover data

Oil palm training data used in this study was obtained from a combined source from previous studies, ground truth data and visual identification of oil palm plantation from high-resolution imagery of CA. Specifically, the existing oil palm layer was obtained from the

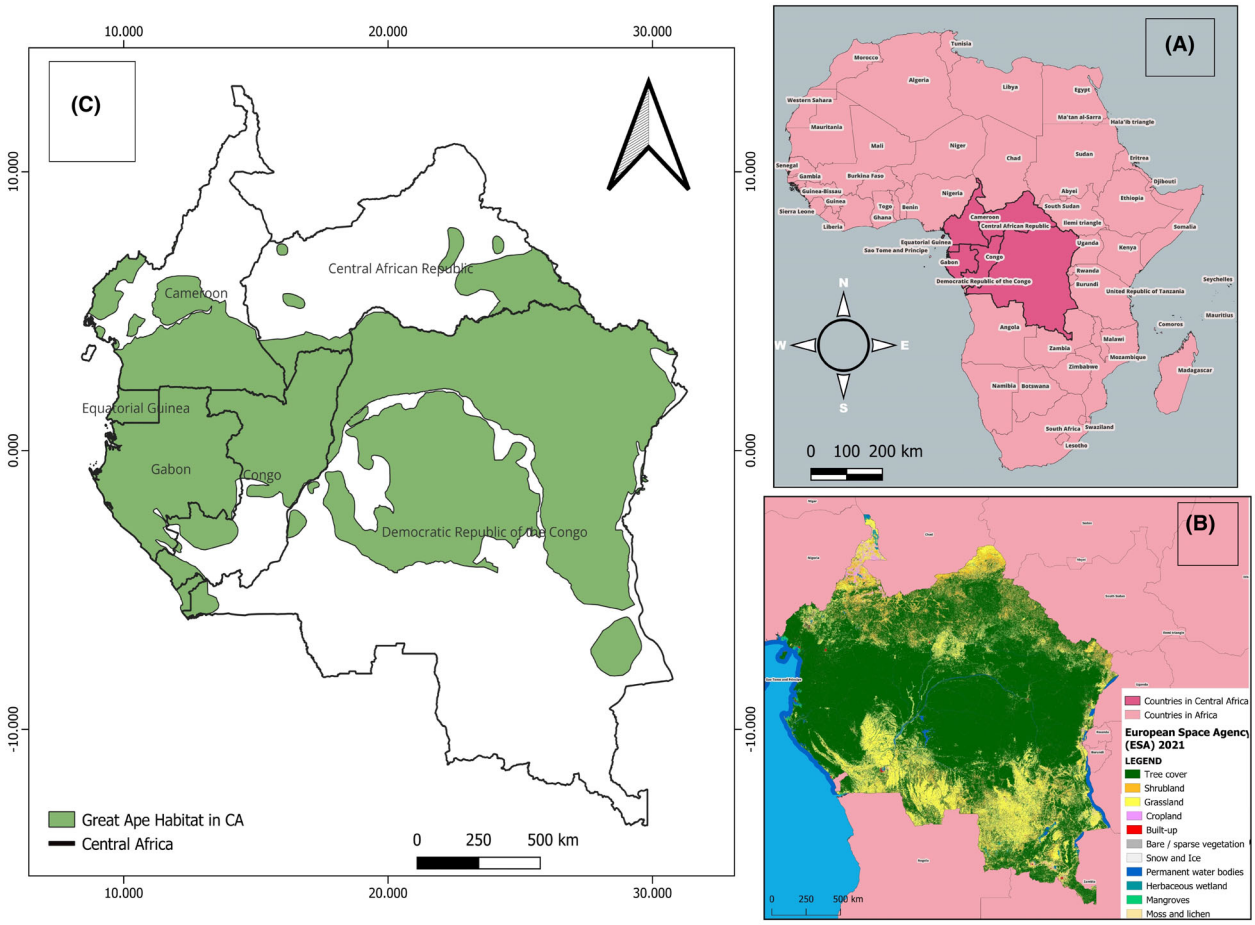

Figure 1. Study area coverage of Central Africa (CA) region with an approximate area of 3 733 000 km^2. (A) The six CA countries (including Central Africa Republic, Republic of Congo, Democratic Republic of Congo, Cameroon, Equatorial Guinea and Gabon around the Congo forest basin) within the Africa Continent. (B) Recent Land cover map for CA from the European Space Agency (ESA) Climate Change Initiative (CCI) Land cover product 2021. (C) The International Union for Conversation of Nature (IUCN) published great ape ranges for CA.

International Union for Conservation of Nature (Meijaard et al., 2018) which shows the industrial oil palm plantations at the global scale. These data were used for initial assessment of oil palm within the CA countries. Furthermore, the predicted oil palm extent from Descals et al. (2021) was used to identify existing oil palm plantations (both industrial and smallholders) to select training sites. A link to this data is provided in the Data Availability Statement.

We employed three classes in this study, namely smallholder oil palm (SOP), industrial oil palm (IOP) and other land (OL). SOP consisted of smaller unit of oil palm plantations typically cultivated within rural and informal settings. Young oil palm, sparse and isolated oil palm were also grouped as SOP, while OL uses such as water, shrubs, mangrove, tropical rainforest, and bare land were categorized as OL. Young oil palm were grouped together with sparse and isolated oil palm owing to the dissimilar characteristics with large oil palm plantations, as most IOP plantation attain maturity at the same time and therefore present the same spectral reflectance characteristics. The IOP consisted of oil palm cultivations associated with industrial level of production. These are large areas of homogeneous oil palm equidistantly separated by roads (Azhar et al., 2015; Descals et al., 2019, 2021; Oon et al., 2019) to form rectangle or other defined regular shapes.

We used the European Commission's Joint Research Centre tropical moist forests (TMF) annual forest cover change map products. The annual change maps comprises of 6 classes (namely: undisturbed tropical moist forest, degraded tropical moist forest, deforested land, forest regrowth, permanent and seasonal water, and other land cover). For the purpose of this study we used the annual change map for the year 2000 and 2021 to establish forest cover change and transition to oil palm at 30-m

resolution. Our forest change analysis and dynamics focused on Undisturbed TMF and Degraded TMF since they both represent areas where the African apes predominantly occur. A link to the TMF JRC data is provided in the Data Availability Statement.

U-Net deep learning model for semantic segmentation

Image segmentation has become an effective and reliable method to extract features from satellite imagery. In this study, we used a U-Net semantic segmentation deep learning model (Ronneberger et al., 2015). The U-Net architecture typically consists of a constricting top to bottom path and a swelling bottom to top path. During the contraction phase, spatial information is compressed while feature information is expanded. The contracting path follows the typical architecture of a convolutional network, where 3 × 3 convolutions (unpadded convolutions) application are repeated twice, then each followed by a rectified linear unit (ReLU) and a 2 × 2 max pooling operation with stride 2 for down sampling. During down sampling, the number of feature channels are doubled and for each step in the extended path an up sampling of the feature map is implemented. This is followed by a 2 × 2 convolution ("up-convolution") that equals the number of feature channels, and a concatenation with the corresponding cropped feature map from the contracting path, as well as a two 3 × 3 convolutions, each followed by a ReLU. At the final layer, a 1 × 1 convolution is used to map each 64-component feature vector to the desired number of classes, at which point the total network added up to a total of 23 convolutional layers.

Analysis and modeling

The training input used for calibrating the U-Net model consists of pairs of images, X and Y, which are the satellite observations (X) and the labeled images (Y), respectively. Labeled images had a fixed dimension of 10-by-10 km^2 generated across selected areas to capture the three major classes (IOP, SOP and OL, classes). The feature of interest was first captured using on-screen digitization of IOP, SOP and OL classes before converting to raster file. The masks were generated in the QGIS environment, comprising at least two classes, and labeled with specific numbers as class labels to obtain the final labeled images (Y). Similarly, the corresponding single Sentinel-1 (VV and VH) and Sentinel-2 (Band 4) satellite image bands based on the preprocessing implemented in Remote Sensing Data (Sentinel-1 and Sentinel-2) section were downloaded from Google Earth Engine (GEE) and layer stacked to generate the satellite image observation (X). The pair of satellite images and labeled images were used for training the U-Net. Figure 2 shows the overall methodological flowchart of this study.

A total of 72 training masks (labeled images) spanning across several SOP and IOP plantations, together with corresponding labels were generated and used for the U-Net deep learning model calibration. We set calibration procedure to consistently use training sites for only calibration and validation samples, while test samples were retained for performance assessment. 75% of the masks was used for calibration, while 15% was used for validation and the remainder of the 10% masks were used for testing the model. The developed U-Net model was thereafter used to predict the respective classes (IOP, SOP and OL) from the Sentinel-1 (VV and VH) and Sentinel-2 (Band 4) final stacked image across the study area. The Sentinel data were a uniform GRID image spanning across the entire extent of the CA with GRID size of 100-by-100 km^2. We evaluated the predicted oil palm layer extents using accuracy assessment as suggested by Olofsson et al. (2014) and Szantoi et al. (2021) to validate the final oil palm layer and assess the performance of the U-Net fused product.

Image classification using U-Net

Three separate U-Net segmentation models were generated and used to predict the target classes (i.e., IOP, SOP and OL, classes). This was done to improve the overall detection rate of the oil palm classes owing to the distinct nature of the crop in CA. The first U-Net image segmentation procedure was an ordinary model which was set to run a total of 300 epochs for model calibration after which the developed model was used to predict the oil palm classes. This procedure particularly enhanced the detection of SOP sites within the study area. The SOP plantation usually relies on local processes to cultivate oil palm around residential neighborhoods or adjacent large scale IOP operators. Given the small scale and less operational requirement for this type of plantation, the farms usually do not have roads interlinking several sections of the farms. They are usually small in area (less than 5 hectares) and without uniform shape or size.

The second model involved the generation of the U-Net model with a data augmentation procedure implemented for training samples. We used data augmentation by rotating the images at an angle of 45°. This increased the number of training site by 24 (Descals et al., 2021). Results from this, characteristically improved the edge detection rate and details of the classified image, especially for the IOP class (in this case), as they typically had distinct shapes (of either rectangular, square or curvilinear) (Descals et al., 2021; Oon et al., 2019). The last

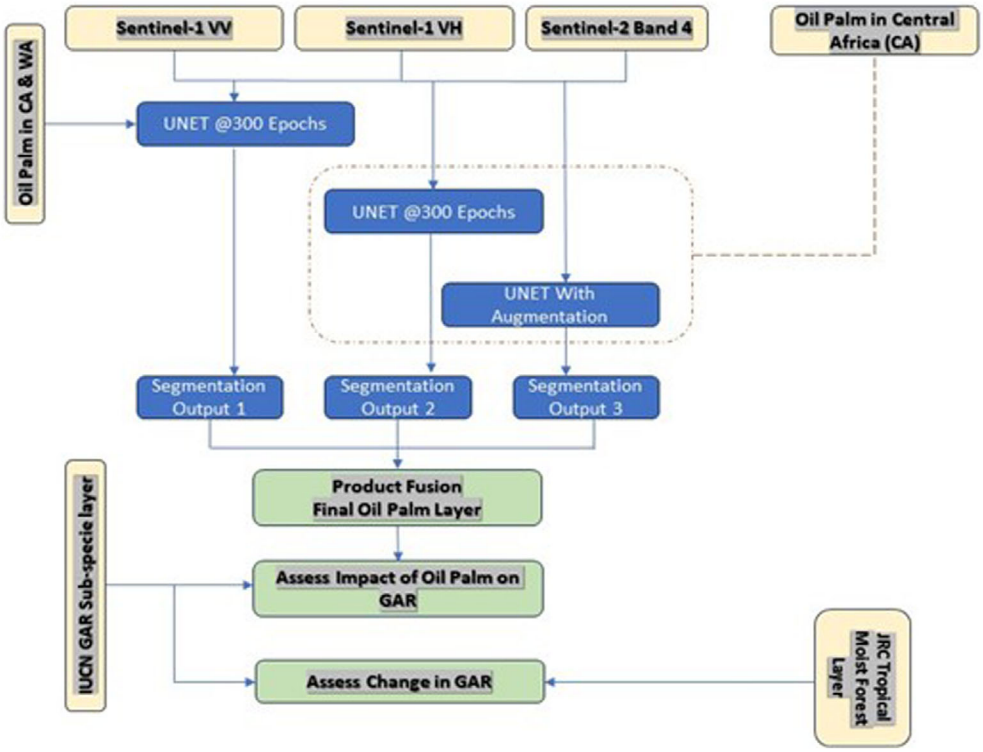

Figure 2. Operational methodological flowchart used in this study.

U-Net segmentation process involved the harmonized use of training sites from within and outside CA to calibrate the U-Net model. In this case, we included ground truth oil palm training data from other west African sites to increase the number of training sites and improve classification accuracy. Similarly previous experiments carried out in this regard also suggest that use of more training sites with substantial diversity improves the detection rates and accuracy, as opposed to when only few training sites are used for classification. Results from these image segmentation processes were thereafter fused (using a simple merge operation in QGIS) to obtain a final oil palm layer for CA. The fusion method integrates layers based on hierarchical importance, where classes at the topmost layer are retained, while classes of the bottom layer compliment the extent of the first layer. This allows for good generalization and expansion of the most predominant class detected in a particular area, especially where the adjacent pixels have the same class.

Image classification using random forest (RF)

In order to assess the performance of the U-Net product fusion, we implemented a machine learning RF classification on the preprocessed Sentinel-1 and Sentinel-2 images for comparison. The RF classification was implemented on the full range of the Sentinel-2 spectral bands and the Sentinel-1 (VV & VH channels) using the same derivative from Remote Sensing Data Section of this study. This operation was implemented on GEE environment using the same training mask extent of IOP, SOP and OL. The RF model works based on tuning two major parameters, namely, the number of trees (*ntree*) in the forest and the number variables in each node (*mtry*). In this study, we calibrated the RF model based on 500 *ntree*, while *mtry* was set to 4 (square root of the total number of the input variable). We also assessed the final output from the RF classification using error matrix and variable importance.

Validation of result

The validation process involved producing error matrix (Congalton, 1991), and the confidence interval as suggested by (Olofsson et al., 2014) before comparing our area mapped and estimates to results of other similar studies. The reference sample data used for the accuracy assessment were selected based on high-resolution satellite image interpretation, verification and assignment of IOP, SOP and OL classes based on output from previous studies (Meijaard et al., 2018). We used HR-Google Earth Image generated over two years (between 2000 and 2022)

for the interpretation, and assignment of the respective target classes. The rationale for this is since oil palm are perennial crops whose existence in a single growing cycle live for more than 15 years. They retain their spatial boundary and remain indifferent for a longtime. This particularly minimized the impact and influence on cloud cover in the image used for sample point interpretation carried out by a single analyst.

A total of 1042 points was generated based on a simple random sampling approach across the oil palm corridor in the CA. A total of 217 points were allocated to IOP class, while 60 points were assigned to the SOP class and a total of 765 points were assigned to OL. The rationale for assigning a higher number of points to the OL is because it has much higher heterogeneity (compared to the IOP and SOP), as it encompasses several land cover classes (such as water, grassland, shrubs, forest, etc.).

The accuracy assessment metrics used to assess the final predicted oil palm layer were the Overall Accuracy (OA), Producer Accuracy (PA) and User Accuracy (UA). Based on the recommendation of Olofsson et al. (2014) good practices for estimating area and assessing accuracy reported we generated the confidence interval. In this study, we utilized a 95% confidence interval for both accuracy metrics and mapped area. In addition, we compared our result for the area coverage of IOP and SOP with outputs from other studies (Cheng et al., 2018; Descals et al., 2021; FAO, 2022).

African ape distribution data

We obtained the African ape distribution data from the International Union for Conservation of Nature (IUCN, 2018) Red List of Threatened Species Database. We extracted spatial data at the sub-specie level for *Pan troglodytes* (Humle et al., 2017), *Pan paniscus* (Fruth et al., 2016), *Gorilla gorilla gorilla* and *Gorilla gorilla Diehli* (Maisels et al., 2018), and *Gorilla beringei beringei* and *Gorilla beringei graueri* (Plumptre et al., 2019). These were subsequently used for assessing forest cover change, and transition between forest cover and oil palm coverage within the African ape distribution in CA.

Results

Predicted class alignment

The results from the image classification as shown in Figures 3A–7, showed a unique characterization of the SOP and IOP classes. The spatial extent of the IOP using the U-Net model had a good topological alignment with the true extent of the oil palm than the output from the RF (Appendix A3) when compared to the high-resolution image in Figure 3B. Our result also indicated substantial presence of SOP and sparsely distributed oil palm units (possibly feral palms) within mixed land cover setting in the region, while other large assemblage of oil palms believed to be old or failed plantations were detected within the IOP.

Accuracy assessment

Accuracy assessment conducted using the 1042 random points presented a 96.4 ± 1.1% overall accuracy (Table 1), indicating a superior performance of the U-Net deep learning model and product image fusion. In contrast, output from the RF had lower OA of 76.3%. The variable importance chart (as shown in Appendices A4 and A5) nevertheless showed that Band-1, Band-12 and VH were the most important variables in the RF classification. Similarly, the producer and user accuracy, which reflects how features on the ground are correctly represented on the classified image and how the map classes are represented on the ground, respectively, also produced high scores for the U-Net model compared to the RF. The IOP class recorded a PA and UA of 91.6 ± 1.7% and 95.0 ± 1.3%, respectively, while the SOP class had PA and UA of 67.7 ± 2.8% and 70.0 ± 2.8%, respectively. Similarly, OL had PA and UA of 99.7 ± 0.3% and 98.4 ± 0.8%, respectively. Conversely, the PA and UA for the RF classification for the IOP was 28.6 and 72.1%, SOP 0 and 0%, and OL 95.8 and 78%, respectively.

In addition, we compared result from the U-Net (with the best output) in two locations with outputs obtained in a previous study (Descals et al., 2021) (Figs. 8 and 9). In general, our approach to mapping oil palm layer using the product fusion helped to spatially capture the entire extent of the IOP as can be seen in Figures 8 and 9.

Area coverage of industrial and small holder OP

Results obtained in this study showed that oil palm covered a total area of 3740 km^2 ± 2000 km^2 as shown in Table 2. Details of the area for IOP and SOP for the six CA countries are also shown in Table 2. SOP in general had a total area coverage of 1290 km^2 ± 400 km^2 (41%), while the IOP plantation had a total area coverage of 2450 km^2 ± 1600 km^2 (59%).

Furthermore, country-based area coverage of combined IOP and SOP extent (as shown in Table 2) indicates that Equatorial Guinea has the least oil palm surface area with a total of 10 km^2 ± 2 km^2 (for both IOP and SOP). Conversely, Cameroon had the highest area of both IOP and SOP, with a total of 1900 km^2 ± 50 km^2.

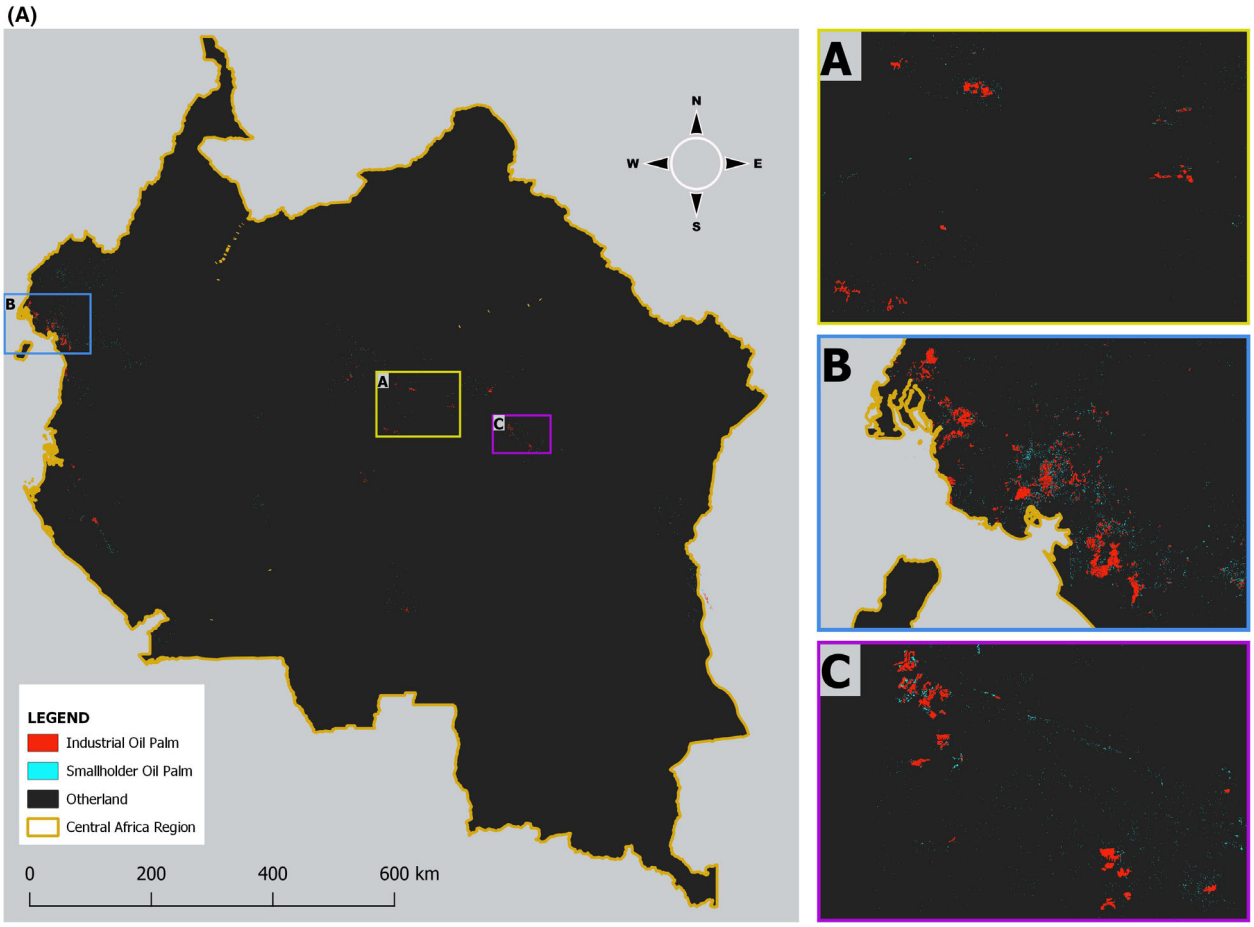

Figure 3. (A) The predicted oil palm layer (IOP and SOP) including Other land cover across Central Africa using a U-Net model and product fusion. (B) Comparison of RF and U-Net predict oil palm (IOP and SOP) including Other land (OL) cover across in three selected locations in Central Africa.

In Gabon, we recorded a total oil palm surface area of 401 km^2 ± 10 km^2. Results obtained in this study also puts the total oil palm area in the Congo as 60 km^2 ± 2 km^2 and in the DRC, we recorded a total of 1390 km^2 ± 40 km^2. In general, results (as shown in Table 3) showed that oil palm cultivation in the six countries combined occupied a total of 5.6% of the total agricultural land for the CA region. We also discovered that oil palm had a less than 1% of the total land cover of the six countries combined.

Assessing the impact of oil palm expansion on forest loss with the African ape distribution

Undisturbed TMF within ranges had reduced significantly by 177 000 km^2 between 2000 and 2021 (Fig. 10 and Appendix A2). Similarly, Table 2 shows the area coverage for the different African great ape ranges. Degraded TMF increased substantially within the 20-years period as a total of 110 000 km^2 of Undisturbed TMF was degraded (i.e., now Degraded TMF), while a total of 60 000 km^2 within the great ape ranges was deforested land and 6000 km^2 was converted to OL. There is a clear indication that 10.40% of the Undisturbed TMF within the great ape natural habitat was converted to either Degraded TMF, Deforested or lost to other land in the 20 years period. Similarly, the results also suggests that c. 5% of great ape habitat (both Undisturbed TMF and Degraded TMF) was completely lost considering that 67 000 km^2 of the Undisturbed TMF could have been converted to Degraded TMF.

Figure 11 presents the result from the comparison (i.e., intersection and extraction) of the forest classes (for 2000) using the oil palm layer (generated for 2021) within the GAR. A total of 1700 km^2 of Undisturbed TMF was

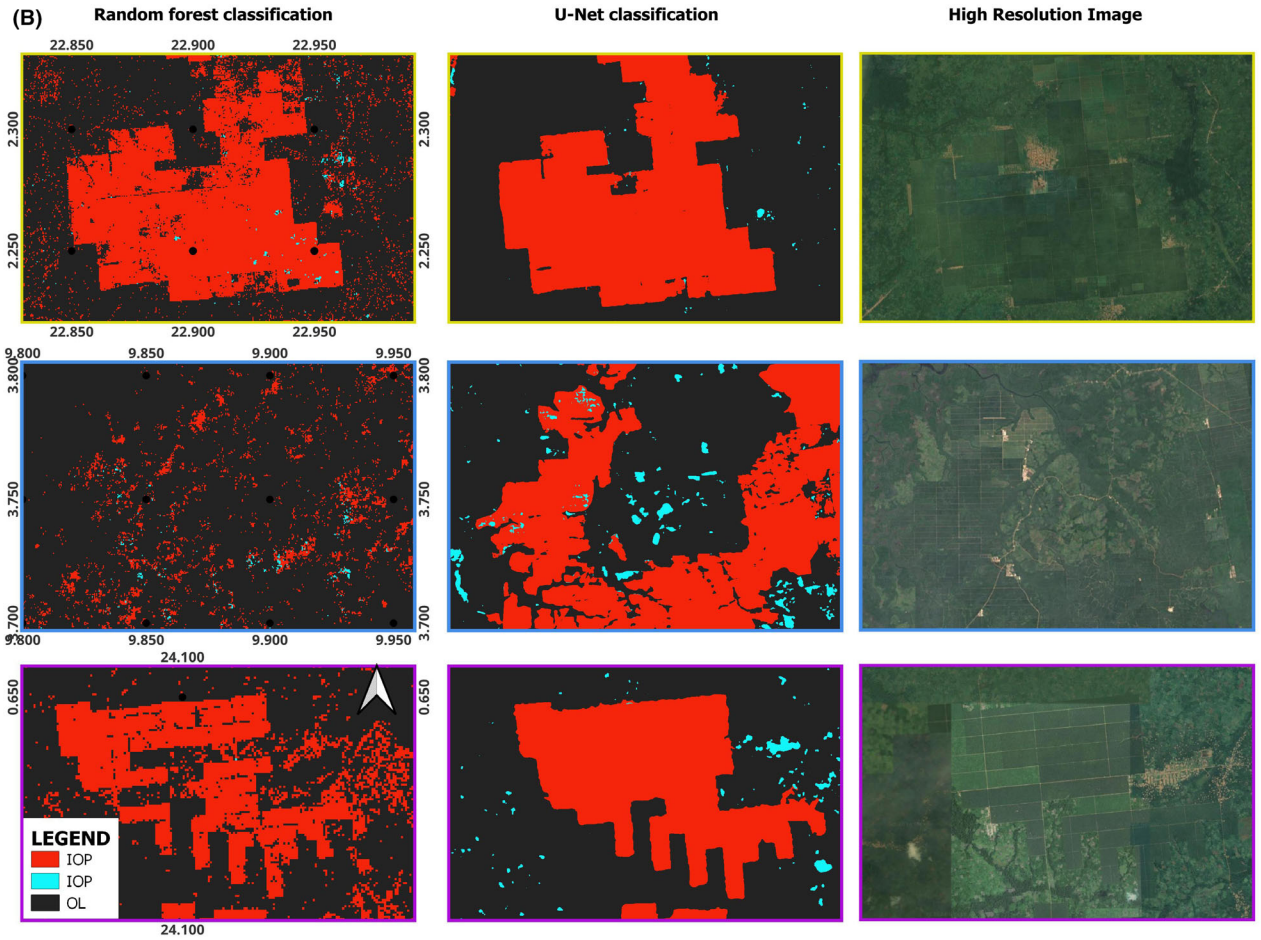

Figure 3. (Continued)

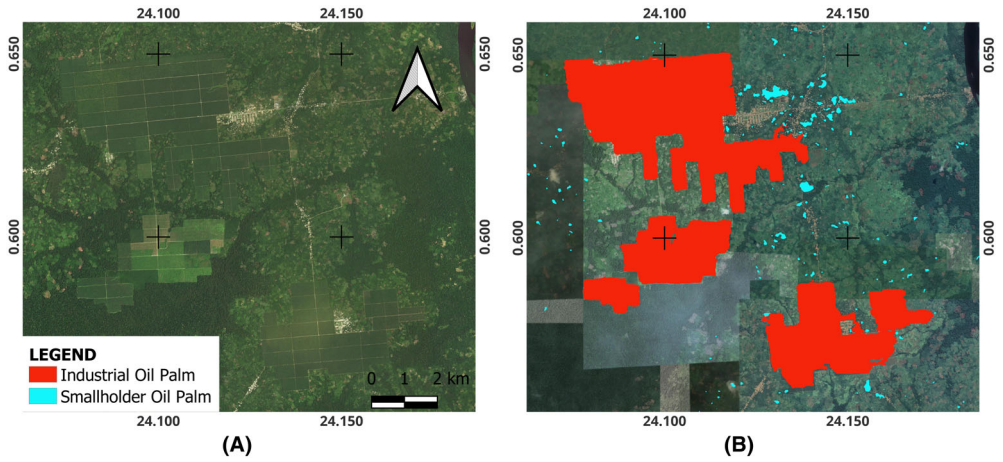

Figure 4. Result of the oil palm layer using the U-Net model and product fusion (A) High-resolution satellite image (B) A predicted IOP and SOP oil palm extent in Democratic Republic of Congo.

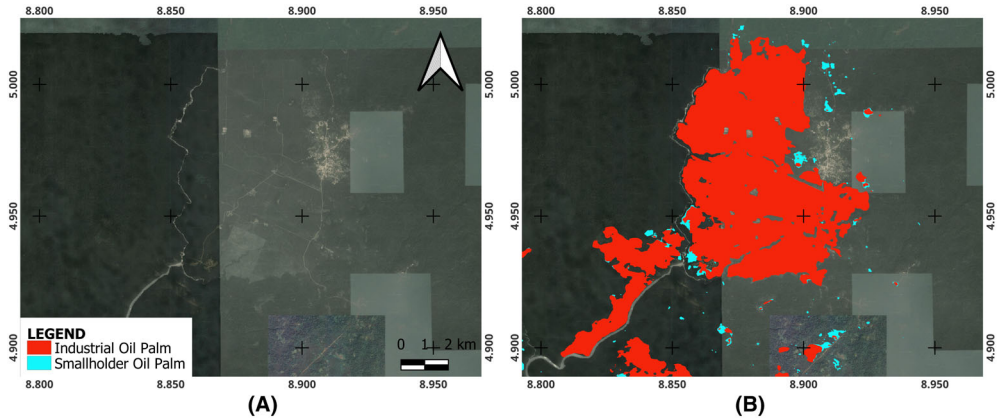

Figure 5. Result of the oil palm layer using the U-Net model and product fusion (A) High-resolution satellite image (B) A predicted IOP and SOP oil palm extent in an oil palm estate in Cameroon.

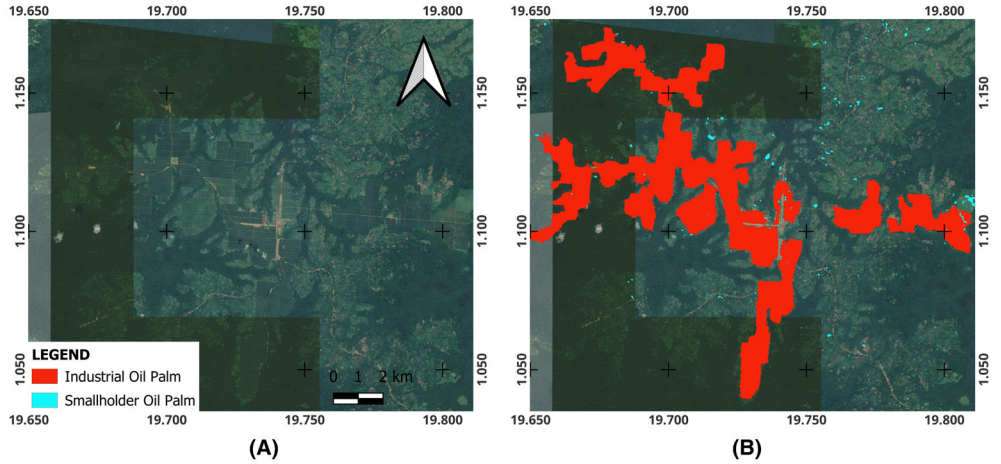

Figure 6. Result of the oil palm layer using the U-Net model and product fusion (A) High-resolution satellite image (B) A predicted IOP and SOP oil palm extent in an oil palm estate in Democratic Republic of Congo. Adjoining rectangle boxes in the images are areas with unresolved pixels in the high-resolution image base map.

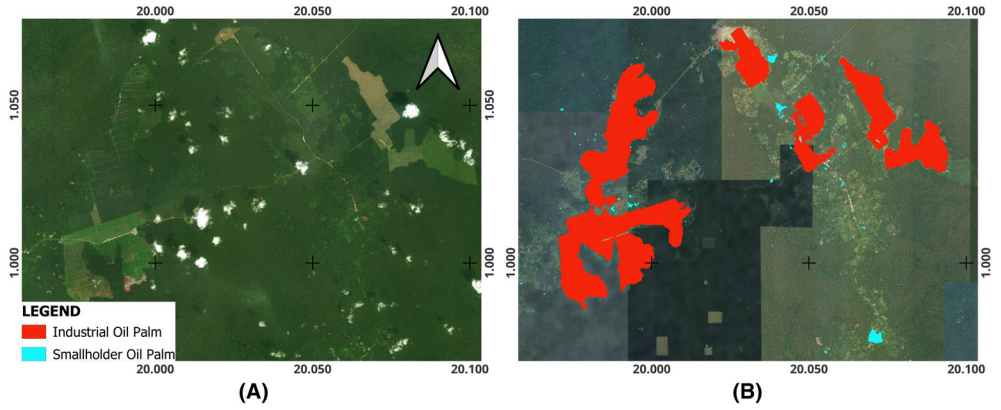

Figure 7. Result of the oil palm layer using the U-Net model and product fusion (A) High-resolution satellite image (B) A predicted IOP and SOP oil palm extent in an oil palm estate in Democratic Republic of Congo. Adjoining rectangle boxes in the images are areas with unresolved pixels in the high-resolution image base map.

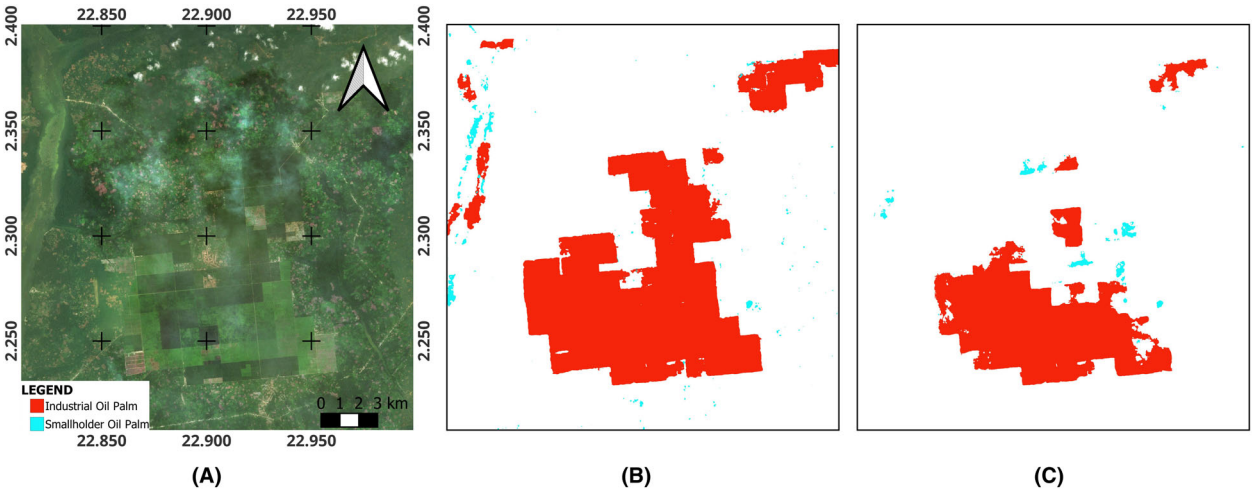

Figure 8. Comparison of the spatial extent of predicted Industrial and smallholder oil palm units in an area in Democratic Republic of Congo. (A) High-resolution satellite imagery of the classification result of industrial and smallholder oil palm (B) Classification result in this study (C) Classification result from Descals et al. (2021).

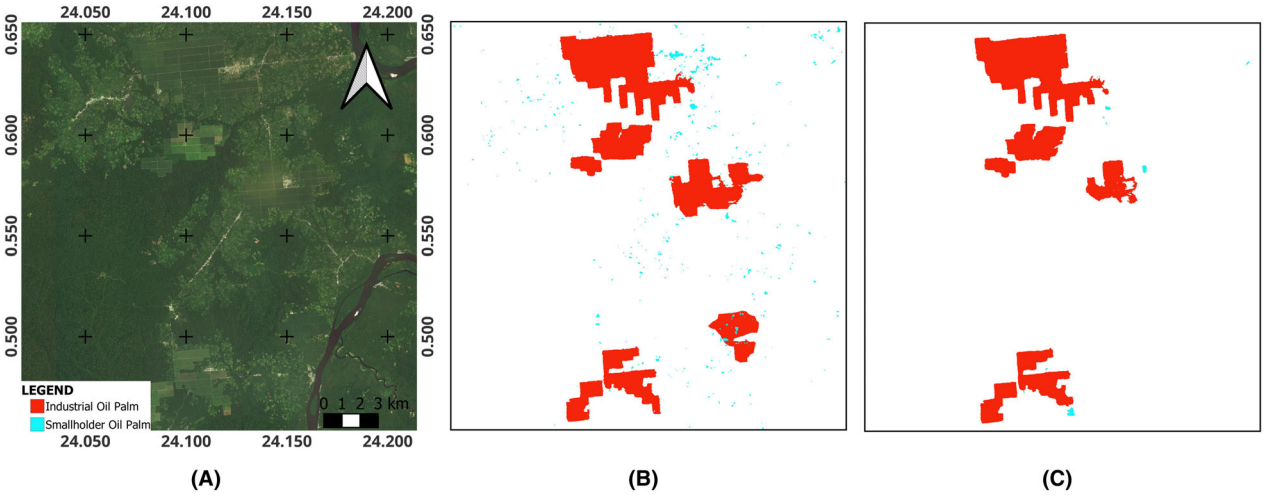

Figure 9. Comparison of the spatial extent of predicted Industrial and smallholder oil palm units in an area in Democratic Republic of Congo. (A) High-resolution satellite imagery of the classification result of industrial and smallholder oil palm (B) Classification result in this study (C) Classification result from Descals et al. (2021).

converted to oil palm by 2021. While 59.8% (1100 km^2) of this was as a result of IOP development, 40.2% was due to establishment of SOP cultivation. In addition, 800 km^2 of oil palm were established in areas classified as deforested land, with 81% being IOP and 19% as SOP. Degraded TMF converted to oil palm had the least coverage (as shown in Fig. 11) with a total area of 120 km^2 for both IOP and SOP.

Furthermore, Figure 12 and Table 4 shows the statistics of forest cover class (for the year 2000) converted to oil palm (generated in this study for 2021) for the various great ape sub-specie ranges. The result evidenced that oil palm induced deforestation or forest degradation (by at least 150 km^2) across the various ranges within the last 20 years. This is as portions of these oil palm cultivation were observed to have been carried out within the undisturbed forest, particularly in the *Pan troglodytes troglodytes*, *Pan troglodytes ellioti*, *Pan troglodytes schweinfurthi* and *Gorilla gorilla* ranges. This led to decline in these subspecies ranges especially *Gorilla gorilla gorilla*, *Pan*

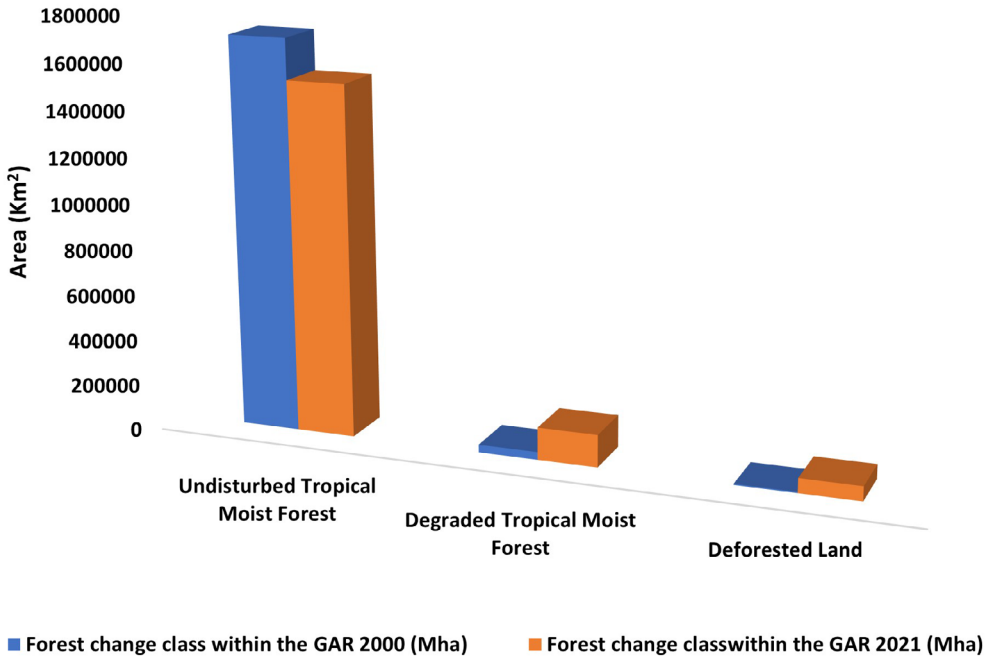

Figure 10. Bar plot showing the area in hectares of Undisturbed TMF, Degraded TMF and Deforested Land for the year 2000 (blue) and 2021 (orange) within the Great Ape Ranges (GAR) of Central Africa (CA). This shows a declining area in Undisturbed TMF due to increasing rate of deforestation and forest degradation within the GAR.

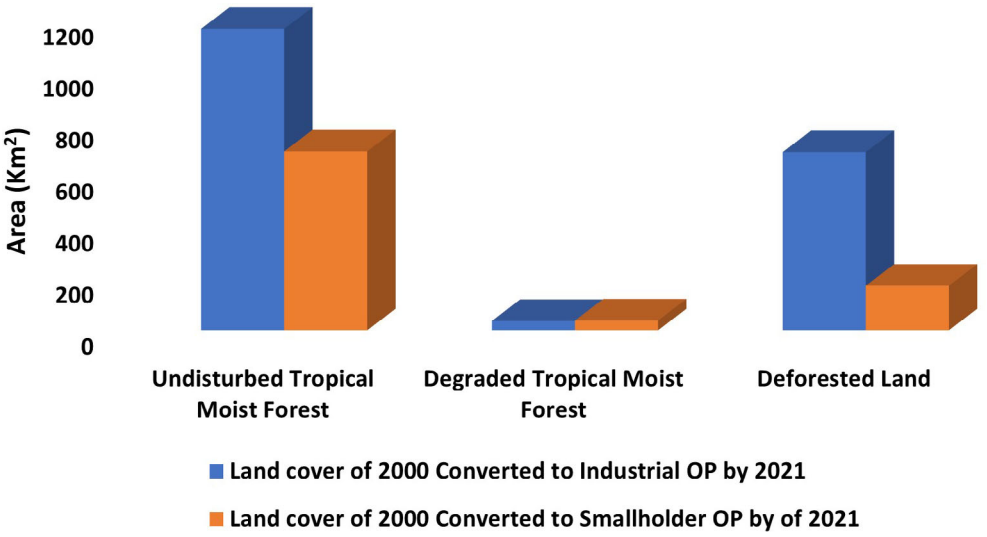

Figure 11. Result of intersection of oil palm layer (both Industrial Oil Palm and Smallholder Oil Palm) with TMF, Degraded TMF, and Deforested land within the International Union for Conservation of Nature (IUCN) great ape ranges to determine forest cover changed to oil palm within the great ape ranges of CA. This suggests that most of the present-day industrial oil palm plantation (totaling to ~1650 km^2) were established within Undisturbed TMF and Deforested Land. Over 600 km^2 of Smallholder oil palm cultivation were also established within Undisturbed TMF leading to degradation of deforestation of the forest cover.

troglodytes troglodytes, *Pan troglodytes schweinfurthi*, and *Pan paniscus* with total losses of 330, 320, 290, and 190 km^2, respectively.

Conversely, the *Gorilla beringei graueri* and *Gorilla gorilla diehli*, had the least decline in their ranges, with area declines of 20 and 2.7 km^2, respectively. A major

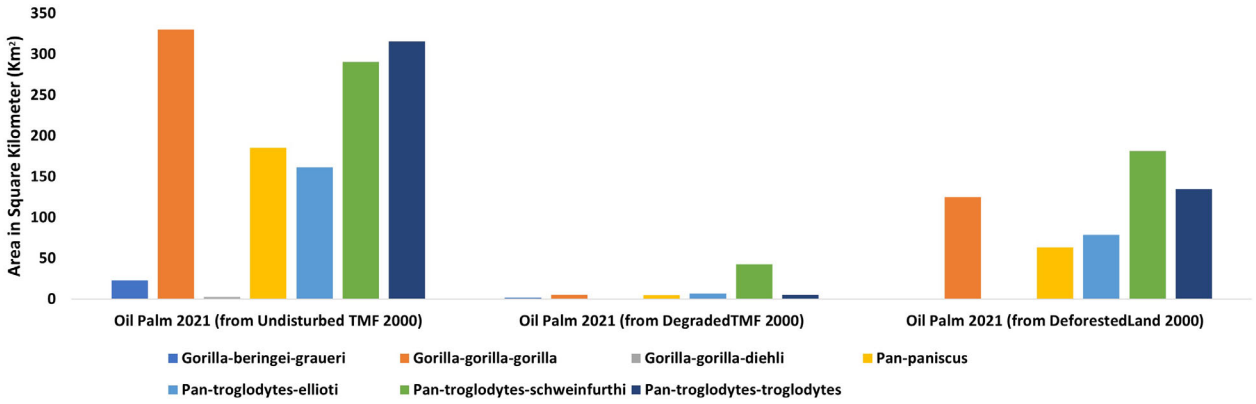

Figure 12. Oil palm impact on great ape ranges. The above figure show forest cover types (Undisturbed TMF, Degraded TMF and Deforested land) converted to oil palm by African great ape ranges. It is evident that most current oil palm cultivation (totaling to at least ~1220 km^2) were once forest covered & great ape ranges but are currently either industrial or smallholder oil palm. This excludes the Gorilla beringei beringei where no evidence of oil palm cultivation was observed.

Table 1. Error matrix obtained from the accuracy assessment. This indicates high overall accuracy, but error of omission (producer accuracy), and commission error (user accuracy) for the SOP. In this case, the columns are the mapped classes, while the rows represent the ground truth. Producer and User accuracies were provided with the 95% Confidence Interval (CI).

Classes	Industrial oil palm	Smallholder oil palm	Other land cover	Total	Producer accuracy (%)	User accuracy (%)
Industrial oil palm	206	11	0	217	91.6 **(89.9, 93.3)**	95 **(93.6, 96.3)**
Smallholder oil palm	16	42	2	60	67.7 **(64.8, 70.5)**	70 **(67.2, 72.8)**
Other land cover	3	9	753	765	99.7 **(99.4, 100.0)**	98.4 **(97.3, 99.5)**

Note: The bolded values are the confidence interval (i.e. plus/minus) of the actual producer accuracy (unbolded values).

Table 2. Total area coverage of smallholder (SOP) and industrial oil palm (IOP) in the six countries of Central Africa. This was also compared with the total harvested area of oil palm reported by the FAO (2022), Cheng et al. (2018), and Descals et al. (2021).

CAR countries	Estimated area (km^2)	IOP (km^2)	SOP (km^2)	FAO (2020) (km^2)	Cheng et al. (2018) (km^2)	Descals et al. (2019) (km^2)
Cameroon	1900 **(1850, 1950)**	1260	590	2200	2710	700
Central African Republic	30 **(28, 32)**	20	10			10
Congo	60 **(58, 62)**	10	50	100	610	12
DR Congo	1390 **(1350, 1430)**	890	500	3200		740
Equatorial Guinea	10 **(8, 12)**		10			3
Gabon	410 **(400, 420)**	270	130	100		140
Total	3740 **(1740, 5740)**	2450	1290	5700		1604

Note: The bolded values are the confidence interval (i.e. plus/minus) of the actual producer accuracy (unbolded values).

reason for the low declines could be due to the high altitude associated with these areas making them less susceptible to habitat conversion into oil palm plantations. However, results also suggests that *Gorilla beringei beringei* range was not affected by oil palm cultivation within the period assessed and as such, was not captured in Figure 12. This results suggests that oil palm expansion has caused a small proportion of the total habitat loss, and thus indicates that other drivers of deforestation are having a bigger impact on the great ape range.

Discussion

This study aimed to map the spatial extent of IOP and SOP (*Elaeis guineensis*) in CA using a U-Net model and image product fusion methodology. Results obtained in

Table 3. Oil palm area as percentage (%) of total agricultural land and total land surface area of each country in CA. Results show that oil palm across the countries occupies land area of less than 2% of any each country of the CA, suggesting that current oil palm cultivation represents small fraction of the entire agricultural activities in the country.

Country	Area of oil palm (km^2)	Agricultural land area (FAO, 2021) (km^2)	Total area of country (km^2)	Oil palm area as percentage of total area of agricultural land (%)	Oil palm area as percentage of total area of country (%)
Cameroon	1850.0	97 500.0	466 544.0	1.90	0.40
CAR	35.7	49 100.0	620 303.8	0.07	0.01
Congo	74.0	106 780.0	340 599.2	0.07	0.02
DRC	1358.9	338 980.0	2 330 344.1	0.40	0.06
Equatorial Guinea	11.9	1049.2	26 959.4	1.13	0.04
Gabon	423.5	21 532.4	264 715.5	1.97	0.16

Table 4. Area coverage of individual African great ape (sub) species in Kilometer Square (km^2) in 2000 and 2021. Evidence from this suggests a decline in the habitat of the great ape ranges.

African great species	Undisturbed TMF 2000 (km^2)	Undisturbed TMF 2021 (km^2)	Degraded TMF 2000 (km^2)	Degraded TMF 2021 (km^2)	Deforested land 2000 (km^2)	Deforested land 2021 (km^2)
Gorilla beringei graueri	46 017	42 452	920	3622	93	825
Gorilla beringei beringei	252	241	6	15	–	2
Gorilla gorilla gorilla	643 129	609 502	3601	28 085	562	8499
Gorilla gorilla diehli	2125	1994	30	126	1	31
Pan paniscus	394 448	365 018	3378	23 768	547	8645
Pan troglodytes ellioti	42 777	37 783	1678	4617	178	2078
Pan trogolodytes schweinfurthii	590 814	489 166	23 971	78 971	3423	42 786
Pan trogolodytes troglodytes	652 376	614 825	4063	31 364	603	9502

this study provided important insights into SOP and IOP expansion in the various countries of the CA, its impact on forest cover, and great ape ranges. Relatively few studies have attempted to map oil palm coverage over CA at a high spatial resolution. Previous attempts have either assessed oil palm coverage for specific countries within the region (Cheng et al., 2018) or as part of a global study (Descals et al., 2021; Du et al., 2022).

With an OA of 96.4% the U-Net model surpassed the RF model classification, which had an OA of 76.4% together with low UA values of zero for the SOP class. A possible reason for the low accuracy from the RF model could be as a result of the unbalanced training sites among classes. This is largely premised on the smaller spatial extent and dispersed nature of SOP compared to IOP and OL which had larger area coverage. This accounted for a corresponding lower number of pixels for the SOP in the training of the RF classifier and also possibly affecting the accuracy of the SOP class.

In this study, we compared our overall classification accuracy (96.4 ± 1.1%) from the U-Net model with results obtained in Descals et al. (2021) (95.1%) and this suggests a difference of 1.3%. Although, given the uncertainties within the reported estimates these variations may not be significant. A major reason for this can be attributed to the use of the product fusion technique, which enabled the integration of multiple predicted oil palm layers (from the three experimental scenarios: (a) normal calibration parameters (b) calibration with data augmentation and (c) calibration using training sites within and outside the CA), and subsequently led to wider area coverage of the final IOP and SOP layer.

The total mapped area of both IOP and SOP (2450 km^2 ± 1600 km^2 and 1290 km^2 ± 400 km^2) obtained in this study was substantially higher than the mapped area of oil palm reported in Descals et al. (2021) 1050 and 550 km^2, respectively, for the CA. While country level comparison with Cheng et al. (2018) showed a

higher mapped area of oil palm for Cameroon (2710 km^2) and Congo (610 km^2). A possible reason for the observed difference in the areas reported in this case could be as a result of the inclusion of young oil palm in the training of the maximum likelihood classifier used in their study. In this case, an accuracy assessment was not conducted for the two countries, and thus prevented a comparison of the accuracy assessment metrics.

A similar comparison with the FAO published oil palm harvested area for the year 2020 (FAO, 2022) showed that the FAO data was higher by ~0.15 km^2 from our mapped coverage of oil palm for the entire CA region. Moreover, our mapped area of oil palm was 400% higher than the FAO reported oil palm harvested area in Gabon, while zero oil palm was reported by FAO in Equatorial Guinea. In the DRC and CAR, our recorded total coverage of oil palm (1390 $km^2 \pm 40$ km^2) and (30 $km^2 \pm 2$ km^2), respectively, were higher than the reported 740 and 10 km^2 area in Descals et al. (2021), but were much lower than the FAO harvested area.

A possible reason for the observed difference could be as a result of the fact that FAO data is self-reported by individual countries, thereby increasing the chance of discrepancies between results obtained from remote sensing application and the FAO recorded harvested area. In this study, we generated training sites base on the boundary of SOP and IOP plantation for calibration of the U-Net model and prediction of the final oil palm layer. This increased our chance of detecting our specific class of interest, while minimizing the chances of detecting artisanal/household level oil palm fields.

Findings from this study, shows that oil palm area constitutes 5.6% of all agricultural land in the region, and is responsible for forest loss of ~1800 km^2 in the 20-year period assessed. This represents 0.9% of the 177 000 km^2 of Undisturbed TMF loss within the great ape ranges, and therefore suggest the assertion (e.g., in Shapiro et al., 2022, Tyukavina et al., 2018) that cropland expansion including for small-scale agriculture could be responsible for the observed high rate of deforestation in this region. Although, our results also did support findings in Vijay et al. (2016) where regional analysis for the Africa continent suggests that 7% of oil palm plantations were observed to have being once forest in 1989, also reinforcing the assertion that oil palm cultivation in the region has witnessed exponential growth through forest clearing.

Furthermore, Meijaard et al. (2018) also noted that considerable variation in circumstances in different settings can lead to wide integration of traditional palm oil producers in mixed cropping systems with large industrial-scale cultivation operating in monocultures and vice-versa, can also influence forest to oil palm conversion. In general, it is believed that small-scale cultivation throughout the region, coupled with accelerated infrastructural development could lead to exponential levels of forest depletion in the Congo forest basin and consequently reducing the natural habitat of great apes.

An evaluation by great ape subspecies ranges showed a loss in Chimpanzee and Gorilla ranges in CA within the last 20 years. We discovered that these and other great ape ranges were reduced by at least ~160 km^2, primarily caused by the direct conversion of forest into oil palm cultivation. This supports findings in previous studies (Carvalho et al., 2021; Strona et al., 2018) where results from model-based prediction signaled potential loss in great ape ranges owing to expansion in oil palm plantation. However, other human induced activities such as logging, agriculture and physical development are also a potential driver of change (Masolele et al., 2024; Shapiro et al., 2022; Tegegne et al., 2016; Tyukavina et al., 2018) leading to substantial decline in this great ape ranges.

While it is possible that the area reduction in these great ape ranges by oil palm development could be higher than as presented in this study, owing to the difference in spatial extent observed in previous studies (Cheng et al., 2018; Descals et al., 2021), and FAO harvested area for countries like Cameroon and Congo. Future studies can focus on improving this outcome by distinguishing among the different species of palms as separate classes and identifying the age of the oil palm stands. This will improve the detection and estimates of oil palm for the region and further highlighting the change dynamics between forest cover and agricultural activities within the CA. Providing the much-needed explanation for the cause of constant forest loss, the essential biodiversity, and endangered species within CA.

Conclusion

This study assessed the potential of a U-Net deep learning model to classify Sentinel-1 (VV, VH) and Sentinel-2 (red band) for the year 2021. The classified image products resulting from this analysis were thereafter fused using a simple product fusion algorithm to generate a regional map of IOP plantation and SOP units for CA. This study provided among other things the first regional scale oil palm map for CA, forest loss within the great ape ranges and further established forest loss owing to oil palm. In general, we observed a great reduction in the Chimpanzee and Gorilla range as deforestation accounted for forest loss of nearly 180 000 km^2 of TMF in the GAR. While it was observed that oil palm conversion to forest may not necessarily be a significant driver of this sharp deforestation (and leading cause of loss of great ape habitat) in the region (as 1700 km^2 of forest was converted to oil palm within the 20 years period examined). It is indeed possible that significant SOP and young oil palm units could have an impact

and influence this forest loss. Further research is certainly needed to help improve our understanding of other drivers, such as small-scale agriculture, infrastructural development in general and the impact on great ape ranges within CA.

Acknowledgments

This research was undertaken with financial support from the United Nation Environmental Programme (UNEP) under the Global Environment Facility (GEF) Congo Basin Impact Program (PCA/2022/5067). We thank Johannes Refisch for providing comments on an earlier version of the paper.

References

Adugna, T., Xu, W. & Fan, J. (2022) Comparison of random forest and support vector machine classifiers for regional land cover mapping using coarse resolution FY-3C images. *Remote Sensing*, **14**, 574.

Alcock, T.D., Salt, D.E., Wilson, P. & Ramsden, S.J. (2022) More sustainable vegetable oil: balancing productivity with carbon storage opportunities. *Science of the Total Environment*, **829**, 154539.

Austin, K.G., Schwantes, A., Gu, Y. & Kasibhatla, P.S. (2019) What causes deforestation in Indonesia? *Environmental Research Letters*, **14**, 024007.

Azhar, B., Saadun, N., Puan, C.L., Kamarudin, N., Aziz, N., Nurhidayu, S. et al. (2015) Promoting landscape heterogeneity to improve the biodiversity benefits of certified palm oil production: evidence from Peninsular Malaysia. *Global Ecology and Conservation*, **3**, 553–561.

Breiman, L. (2001) Random forests. *Machine Learning*, **45**, 5–32.

Carvalho, J.S., Graham, B., Bocksberger, G., Maisels, F., Williamson, E.A., Wich, S. et al. (2021) Predicting range shifts of African apes under global change scenarios. *Diversity and Distributions*, **27**, 1663–1679.

Cheng, Y., Yu, L., Xu, Y., Liu, X., Lu, H., Cracknell, A.P. et al. (2018) Towards global oil palm plantation mapping using remote-sensing data. *International Journal of Remote Sensing*, **39**, 5891–5906.

Congalton, R.G. (1991) A review of assessing the accuracy of classifications of remotely sensed data. *Remote Sensing of Environment*, **37**, 35–46.

Corley, R. & Tinker, P. (2016) *The oil palm*, 5th edition. Chichester: The Atrium, Southern Gate.

Corley, R.H.V. & Tinker, P.B. (2008) *The oil palm*. Oxford: John Wiley and Sons.

Cortes, C. & Vapnik, V. (1995) Support-vector networks. *Machine Learning*, **20**, 273–297.

Curtis, P., Slay, C., Harris, N., Tyukavina, A. & Hansen, M. (2018) Classifying drivers of global forest loss. *Science*, **361**, 1108–1111.

Danylo, O., Pirker, J., Lemoine, G., Ceccherini, G., See, L., Mccallum, I. et al. (2021) A map of the extent and year of detection of oil palm plantations in Indonesia, Malaysia and Thailand. *Scientific Data*, **8**, 96.

Descals, A., Szantoi, Z., Meijaard, E., Sutikno, H., Rindanata, G. & Wich, S. (2019) Oil palm (*Elaeis guineensis*) mapping with details: smallholder versus industrial plantations and their extent in Riau, Sumatra. *Remote Sensing*, **11**, 2590.

Descals, A., Wich, S., Meijaard, E., Gaveau, D.L., Peedell, S. & Szantoi, Z. (2021) High-resolution global map of smallholder and industrial closed-canopy oil palm plantations. *Earth System Science Data*, **13**, 1211–1231.

Drusch, M., Del Bello, U., Carlier, S., Colin, O., Fernandez, V., Gascon, F. et al. (2012) Sentinel-2: ESA's optical high-resolution mission for GMES operational services. *Remote Sensing of Environment*, **120**, 25–36.

Du, Z., Yu, L., Yang, J., Xu, Y., Chen, B., Peng, S. et al. (2022) A global map of planting years of plantations. *Scientific Data*, **9**, 141.

FAO. (2020) *Vegetable oil production, World*. Available from: https://ourworldindata.org/grapher/vegetable-oil-production [Accessed 14th July 2023].

FAO (2021) *Food and agriculture organisation. Area of agricultural land*. Available from: https://fao.org/faostat/en/#data/RL [Accessed 3rd June 2023].

FAO. (2022) *Food and Agriculture Organisation*. Available from: https://www.fao.org/faostat/en/#data [Accessed 21st April 2024].

Feintrenie, L. (2014) Agro-industrial plantations in Central Africa, risks and opportunities. *Biodiversity and Conservation*, **23**, 1577–1589.

Fruth, B.I., Hickey, J.R., Andre, C., Furuichi, T., Hart, J., Hart, T. et al. (2016) Pan paniscus (errata version published in 2016) The IUCN Red List of Threatened Species 2016: e.T15932A102331567. https://dx.doi.org/10.2305/IUCN.UK.2016-2.RLTS.T15932A17964305.en. [Accessed 19th March 2023].

Gaveau, D.L., Locatelli, B., Salim, M.A., Yaen, H., Pacheco, P. & Sheil, D. (2019) Rise and fall of forest loss and industrial plantations in Borneo (2000–2017). *Conservation Letters*, **12**, e12622.

Ghosh, S., Das, N., Das, I. & Maulik, U. (2019) Understanding deep learning techniques for image segmentation. *ACM Computing Surveys (CSUR)*, **52**, 1–35.

GRASP. (2018) Convention on international trade in endangered species of wild fauna and flora. In: *Seventieth Meeting of the Standing Committee Rosa Khutor, Sochi (Russian Federation), 1–5 October 2018*, SC70 Doc. 52. https://cites.org/sites/default/files/eng/com/sc/70/E-SC70-52.pdf [Accessed 12th October 2023].

GRASP. (2023) Convention on international trade in endangered species of wild fauna and flora. In: COP18, R. O. T. I. O. R. C. R. (ed.). In: *Seventy-Seventh Meeting of the*

Standing Committee Geneva (Switzerland), 6–10 November 2023. https://cites.org/sites/default/files/documents/SC/77/agenda/E-SC77-64.pdf [Accessed 12th October 2023].

Hansen, M.C., Potapov, P.V., Moore, R., Hancher, M., Turubanova, S.A., Tyukavina, A. et al. (2013) High-resolution global maps of 21st-century forest cover change. *Science*, **342**, 850–853.

Humle, T., Maisels, F., Oates, J.F., Plumptre, A. & Williamson, E.A. (2017) *Pan troglodytes*. The IUCN Red List of Threatened Species 2016: e.T15933A102326672. http://dx.doi.org/10.2305/IUCN.UK.2016-2.RLTS.T15933A17964454.en [Accessed 19th March 2023].

International Union for Conservation of Nature. (2018). https://www.iucnredlist.org/species/39999/176396749 Gorilla beringei ssp. beringei (amended version of 2018 assessment). The IUCN Red List of Threatened Species 2020: e.T39999A176396749. https://dx.doi.org/10.2305/IUCN.UK.2020-3.RLTS.T39999A176396749.en [Accessed 19th March 2023].

Kalustian, P. (1985) Pharmaceutical and cosmetic uses of palm and lauric products. *Journal of the American Oil Chemists' Society*, **62**, 431–433.

Lai, O.-M., Tan, C.-P. & Akoh, C.C. (2015) *Palm oil: production, processing, characterization, and uses*. Urbana, IL: Elsevier.

Maisels, F., Bergl, R.A. & Williamson, E.A. (2018) *Gorilla gorilla (amended version of 2016 assessment). The IUCN Red List of Threatened Species 2018*. Gland, Switzerland: International Union for Conservation of Nature (IUCN). Available from: https://doi.org/10.2305/IUCN.UK.2018-2.RLTS.T9404A136250858.en

Margono, B.A., Potapov, P.V., Turubanova, S., Stolle, F. & Hansen, M.C. (2014) Primary forest cover loss in Indonesia over 2000–2012. *Nature Climate Change*, **4**, 730–735.

Masolele, R.N., Marcos, D., De Sy, V., Abu, I.-O., Verbesselt, J., Reiche, J. et al. (2024) Mapping the diversity of land uses following deforestation across Africa. *Scientific Reports*, **14**, 1681.

Meijaard, E. (2021) Borneo Futures. *Global oil palm map*. Available from: https://doi.org/10.5061/dryad.ghx3ffbn9 [Accessed 20th March 2023].

Meijaard, E., Garcia-Ulloa, J., Sheil, D., Wich, S., Carlson, K., Juffe-Bignoli, D. et al. (2018) *Oil palm and biodiversity: a situation analysis by the IUCN Oil Palm Task Force*. Available from: https://portals.iucn.org/library/sites/library/files/documents/2018-027-En.pdf. [Accessed 20 March 2023].

Meijaard, E. & Sheil, D. (2019) The moral minefield of ethical oil palm and sustainable development. *Frontiers in Forests and Global Change*, **2**, 22.

Mhanna, S., Halloran, L.J., Zwahlen, F., Asaad, A.H. & Brunner, P. (2023) Using machine learning and remote sensing to track land use/land cover changes due to armed conflict. *Science of the Total Environment*, **898**, 165600.

Minaee, S., Boykov, Y., Porikli, F., Plaza, A., Kehtarnavaz, N. & Terzopoulos, D. (2021) Image segmentation using deep learning: a survey. *IEEE Transactions on Pattern Analysis and Machine Intelligence*, **44**, 3523–3542.

Naidu, L. (2006) *Manual, soil-site suitability criteria for major crops*. University of Chicago, USA: National Bureau of Soil Survey and Land Use Planning, ICAR.

Noojipady, P., Morton, C.D., Macedo, N.M., Victoria, C.D., Huang, C., Gibbs, K.H. et al. (2017) Forest carbon emissions from cropland expansion in the Brazilian Cerrado biome. *Environmental Research Letters*, **12**, 025004.

Olofsson, P., Foody, G.M., Herold, M., Stehman, S.V., Woodcock, C.E. & Wulder, M.A. (2014) Good practices for estimating area and assessing accuracy of land change. *Remote Sensing of Environment*, **148**, 42–57.

Oon, A., Ngo, K.D., Azhar, R., Ashton-Butt, A., Lechner, A.M. & Azhar, B. (2019) Assessment of ALOS-2 PALSAR-2L-band and Sentinel-1 C-band SAR backscatter for discriminating between large-scale oil palm plantations and smallholdings on tropical peatlands. *Remote Sensing Applications: Society and Environment*, **13**, 183–190.

Ozigis, M.S., Kaduk, J.D. & Jarvis, C.H. (2019) Mapping terrestrial oil spill impact using machine learning random forest and Landsat 8 OLI imagery: a case site within the Niger Delta region of Nigeria. *Environmental Science and Pollution Research*, **26**, 3621–3635.

Ozigis, M.S., Kaduk, J.D., Jarvis, C.H., Da Conceição Bispo, P. & Balzter, H. (2020) Detection of oil pollution impacts on vegetation using multifrequency SAR, multispectral images with fuzzy forest and random forest methods. *Environmental Pollution*, **256**, 113360.

Pande, G., Akoh, C.C. & Lai, O.M. (2012) Food uses of palm oil and its components. *Palm Oil*, **2012**, 561–586.

Plumptre, A., Robins, M.M. & Williamson, E.A. (2019) *Gorilla beringei. The IUCN red list of threatened species* 2019: e.T39994A115576640. https://doi.org/10.2305/IUCN.UK.2019-1.RLTS.T39994A115576640.en [Accessed 23rd August 2024].

Rodríguez, A.C., D'aronco, S., Schindler, K. & Wegner, J.D. (2021) Mapping oil palm density at country scale: an active learning approach. *Remote Sensing of Environment*, **261**, 112479.

Ronneberger, O., Fischer, P. & Brox, T. (2015) U-Net: convolutional networks for biomedical image segmentation. In: *Medical Image Computing and Computer-Assisted Intervention–MICCAI 2015: 18th International Conference, Munich, Germany, October 5–9, 2015, Proceedings, Part III 18*. Switzerland: Springer International Publishing, pp. 234–241.

Shadman Roodposhti, M., Aryal, J., Lucieer, A. & Bryan, B.A. (2019) Uncertainty assessment of hyperspectral image classification: deep learning vs. random forest. *Entropy*, **21**, 78.

Shapiro, A., D'annunzio, R., Jungers, Q., Desclée, B., Kondjo, H., Iyanga, J.M. et al. (2022) *Are Deforestation and*

Degradation in the Congo Basin on the Rise? An Analysis of Recent Trends And Associated Direct Drivers. https://doi.org/10.21203/rs.3.rs-2018689/v1.

Shapiro, A.C., Grantham, H.S., Aguilar-Amuchastegui, N., Murray, N.J., Gond, V., Bonfils, D. et al. (2021) Forest condition in The Congo Basin for the assessment of ecosystem conservation status. *Ecological Indicators*, **122**, 107268.

Strona, G., Stringer, S.D., Vieilledent, G., Szantoi, Z., Garcia-Ulloa, J. & Wich, S.A. (2018) Small room for compromise between oil palm cultivation and primate conservation in Africa. *Proceedings of the National Academy of Sciences*, **115**, 8811–8816.

Su, Q., Tao, W., Mei, S., Zhang, X., Li, K., Su, X. et al. (2021) Landslide susceptibility zoning using C5. 0 decision tree, random forest, support vector machine and comparison of their performance in a coal mine area. *Frontiers in Earth Science*, **9**, 781472.

Szantoi, Z., Jaffrain, G., Gallaun, H., Bielski, C., Ruf, K., Lupi, A. et al. (2021) Quality assurance and assessment framework for land cover maps validation in the Copernicus Hot Spot Monitoring activity. *European Journal of Remote Sensing*, **54**, 538–557.

Tegegne, Y.T., Lindner, M., Fobissie, K.A.N.D. & Kanninen, M. (2016) Evolution of drivers of deforestation and forest degradation in the Congo Basin forests: exploring possible policy options to address forest loss. *Land Use Policy*, **51**, 312–324.

Thanh Noi, P.A.N.D. & Kappas, M. (2017) Comparison of random forest, k-nearest neighbor, and support vector machine classifiers for land cover classification using Sentinel-2 imagery. *Sensors*, **18**, 18.

Tyukavina, A., Hansen, M.C., Potapov, P., Parker, D., Okpa, C., Stehman, S.V. et al. (2018) Congo Basin forest loss dominated by increasing smallholder clearing. *Science Advances*, **4**, eaat2993.

UNESCO. (2020) *United Nations educational scientific and cultural organization protecting great apes and their habitats*. Available from: https://en.unesco.org/themes/biodiversity/great-apes [Accessed 3rd June 2023].

Van der Werf, G.R., Morton, D.C., Defries, R.S., Olivier, J.G., Kasibhatla, P.S., Jackson, R.B. et al. (2009) CO2 emissions from forest loss. *Nature Geoscience*, **2**, 737–738.

Vancutsem, C., Achard, F., Pekel, J.-F., Vieilledent, G., Carboni, S., Simonetti, D. et al. (2021) Long-term (1990–2019) monitoring of forest cover changes in the humid tropics. *Science Advances*, **7**, eabe1603.

Veloo, R., Ranst, E.V. & Selliah, P. (2015) Peat characteristics and its impact on oil palm yield. *NJAS: Wageningen Journal of Life Sciences*, **72**, 33–40.

Vijay, V., Pimm, S.L., Jenkins, C.N. & Smith, S.J. (2016) The impacts of oil palm on recent deforestation and biodiversity loss. *PLoS One*, **11**, e0159668.

Wich, S.A., Garcia-Ulloa, J., Kühl, H.S., Humle, T., Lee, J.S. & Koh, L.P. (2014) Will oil palm's homecoming spell doom for Africa's great apes? *Current Biology*, **24**, 1659–1663.

Wijedasa, L.S., Jauhiainen, J., Könönen, M., Lampela, M., Vasander, H., Leblanc, M.C. et al. (2017) Denial of long-term issues with agriculture on tropical peatlands will have devastating consequences. *Global Change Biology*, **23**, 977–982.

Worldbank. (2020). https://climateknowledgeportal.worldbank.org/country/central-african-republic/climate-data-historical

WWF. (2009) *Unsustainable logging threatens great ape populations*. https://wwf.panda.org/wwf_news/?174101/Unsustainable-Logging-Threatens-Great-Ape-Populations [Accessed 3rd June 2023].

Xu, S., Zhao, Q., Yin, K., Zhang, F., Liu, D. & Yang, G. (2019) Combining random forest and support vector machines for object-based rural-land-cover classification using high spatial resolution imagery. *Journal of Applied Remote Sensing*, **13**, 014521.

Yomo, M., Yalo, E.N., Gnazou, M.D.T., Silliman, S., Larbi, I. & Mourad, K.A. (2023) Forecasting land use and land cover dynamics using combined remote sensing, machine learning algorithm and local perception in the Agoènyivé plateau, Togo. *Remote Sensing Applications: Society and Environment*, **30**, 100928.

Zafar, Z., Zubair, M., Zha, Y., Fahd, S. & Nadeem, A.A. (2024) Performance assessment of machine learning algorithms for mapping of land use/land cover using remote sensing data. *The Egyptian Journal of Remote Sensing and Space Sciences*, **27**(2), 216–226.

Supporting Information

Additional supporting information may be found online in the Supporting Information section at the end of the article.

Appendix A1. Map of the great ape ranges and Habitat as obtained from the IUCN Redlist of Endangered Species Database

Appendix A2. The annual change forest cover maps for the year 2000 and 2021, as obtained from the European Commission's Joint Research Centre website (See Section 13 for full link)

Appendix A3. Predicted Oil Palm Layer for Central Africa using Random Forest Method

Appendix A4. Raw Variable Importance Chart from the Random Forest Classification Using Sentinel-1 (VV & VH) and Sentinel-2 Spectral Bands

Appendix A5. Normalized Variable Importance Chart from the Random Forest Classification Using Sentinel-1 (VV & VH) and Sentinel-2 Spectral Bands

Appendix A6. Error Matrix from the Random Forest Classification of Sentinel-1 (VV & VH) and Sentinel-2 Spectral Bands